

Article

Study on the Force Model of Squeezed Branch Piles Based on Surface Potential Characteristics

Siqing Zhang ^{1,2}, Xiaofei Liu ^{1,2,*} , Huajie Zhang ^{1,2}, Chunde Piao ³ and Yue Niu ^{1,2}

¹ Key Laboratory of Gas and Fire Control for Coal Mines, China University of Mining and Technology, Ministry of Education, Xuzhou 21116, China

² School of Safety Engineering, China University of Mining and Technology, Xuzhou 221116, China

³ School of Resources and Geosciences, China University of Mining and Technology, Xuzhou 221116, China

* Correspondence: liuxiaofei@cumt.edu.cn

Abstract: Squeezed branch piles, which boast the advantages of great bearing capacity, small settlement, and good stability, are an important infrastructure in the foundation of buildings, and their safety state is related to the safety of the entire structure. As a non-destructive testing method, surface potential can be used to effectively evaluate the damaged state of a pile foundation without destroying its stability. On this basis, in this study, the characteristics of surface potential change during settlement and deformation of squeezed branch piles under graded loading were tested and analyzed with the aid of a self-made loading system of reaction beams and an LB-IV multi-channel potential data acquisition system. The results show that: Under graded loading, squeezed branch piles can produce surface potential signals whose intensity can well reflect the settlement and local failure characteristics of the pile foundation; The potential signals change in advance of load; and they fluctuate violently before local fracturing of squeezed branch piles. The unstable fluctuation of the potential signal can be regarded as a precursor to the fracturing of squeezed branch piles. The research results have positive theoretical significance and important application value for assessing the stability of both branch piles and their stress states on site and monitoring and forecasting the disaster of pile foundation instability.

Keywords: graded loading; squeezed branch piles; surface potential; precursor feature; force model



Citation: Zhang, S.; Liu, X.; Zhang, H.; Piao, C.; Niu, Y. Study on the Force Model of Squeezed Branch Piles Based on Surface Potential Characteristics. *Buildings* **2023**, *13*, 2231. <https://doi.org/10.3390/buildings13092231>

Academic Editor: Francisco López-Almansa

Received: 2 August 2023

Revised: 20 August 2023

Accepted: 30 August 2023

Published: 1 September 2023



Copyright: © 2023 by the authors. Licensee MDPI, Basel, Switzerland. This article is an open access article distributed under the terms and conditions of the Creative Commons Attribution (CC BY) license (<https://creativecommons.org/licenses/by/4.0/>).

1. Introduction

As a new form of pile foundation, squeezed branch piles evolved from the traditional equal-section bored pile according to the bionic principle (root structure). Compared with conventional cast-in-place piles, they have the advantages of improving the bearing capacity of the pile foundation, reducing settlement, lowering engineering costs (saving cost), and shortening the construction period [1–3], which is in line with the concept of double carbon development [4]. In the early 1990s, squeezed branch piles were widely used in China. At present, they have been successfully applied to the top 100 projects in more than ten provinces and cities in China, involving electric power construction, municipal engineering, roads and bridges, residential buildings, and so on [5].

The instability of squeezed branch piles is closely related to the development state and evolution process of fractures during a pile failure under load. Domestic and foreign scholars have carried out a lot of research on branch piles. Prateep Lueprasert reveals the pile-soil-tunnel interaction mechanism behind tunnel deformation behavior by studying the influence of buildings with pile foundations on tunnels [6]. Su Qingqing used numerical simulation analysis and concluded that the appropriate number and spacing of the branches would maximize the bearing capacity of the branch pile and reduce the settlement [7]. Zhang Minxia et al. analyzed the influence of branch position, spacing, number, and diameter on pile bearing capacity through numerical simulation, as well as the bearing behavior and failure mechanism of squeezed branch piles [8]. At present, although some

progress has been made in theoretical research on squeezed branch piles, because of the complex loading mechanism of squeezed branch piles, the derivation of theoretical models remains difficult, and various modes of destruction exist. Against this background, the deformation and failure characteristics of squeezed branch piles have become the focus of attention and research in the engineering field [9,10].

During the loading of coal, rock, and concrete, the release of stress accumulated in the sample will lead to pile failure. In this process, energy dispersion often leads to physical anomalies, including electromagnetic anomalies [11,12], acoustic emission [13–16], and infrared effects [17–19], in the sample and its surrounding environment. Potential signaling, as a phenomenon of free charge generation and transfer during deformation or fracturing of concrete and rock under load, is an effective tool for studying damage and fracture evolution of materials. It can monitor the process of crack initiation and expansion dynamically and continuously in real time without destroying the integrity of materials. The research and application of potential, a dynamic monitoring technology, mainly focus on the following two aspects: (1) obtaining the critical precursor characteristics of sample crack expansion based on the characteristic curve of potential signal variation for disaster monitoring and early warning; (2) studying the relationship between potential change and sample fracturing during sample crack expansion for evaluating the damage degree of the sample.

Numerous studies have been conducted on the relationship between the potential signal and stress of loaded materials, the potential response characteristics of crack development and evolution, etc., based on which the damage state of samples has been evaluated. Liu et al. [20] studied the electric potential of the concrete hole wall under uniaxial compression. The results show that potential signals change in advance of load and that the sudden increase in potential signal and the sudden change in potential amplitude increment can be regarded as precursor features of concrete fracturing. The experimental results provide a reference for the use of potential signals for non-destructive testing of concrete damage and destruction processes. Wang et al. [21] believed that the mechanical and electrical phenomena of coal and rock are the electromagnetic effects produced by the relaxation of separated charges in rock under the action of stress. Niu et al. [22] experimentally investigated the electrical charge variations of granite and coal under uniaxial compression, revealing that both rock and coal produced charges when they failed. When studying potential signal variations during surface crack expansion of various concrete and coal rock samples, Li et al. [23,24] observed that surface potential was generated during deformation and fracturing of the samples and that the magnitude of surface potential agreed well with the degree of fracturing and the variation of load. And the surface potential signal has a more obvious response to the rupture, especially in the incubation stage before the main rupture occurs. Previous studies were mostly focused on the surface potential characteristics and variation laws of small-scale rock, coal, and concrete samples during their failure under load in a laboratory [23–25]. However, there is a lack of further study on the damage state of pile foundations, especially on the non-destructive method of testing pile foundation damage. Most disasters due to pile foundation instability in construction projects begin with initial crack expansion. Under the action of load, the continuous development of damages such as micro-crack closure, micro-crack generation, cracking, and failure during the development of fractures in concrete (the main medium of pile foundation) is the root cause of potential change.

At present, static load testing is the most stable and important method to determine the bearing capacity of a pile foundation. At the same time, the indoor model test can be flexibly designed according to the requirements. On the one hand, various performance tests can be carried out by using modern monitoring equipment, and on the other hand, small-scale tests can be carried out to save costs [26]. This paper passed the static load model test of squeezed branch piles, studied the relationship and variation law between the surface potential variation of the concrete pile foundation and the load and the concrete material under the load state of the pile top, investigated stress changes of squeezed branch

piles and surface potential response characteristics, established a loading system and a potential data acquisition system for squeezed branch piles under laboratory conditions, and analyzed the response characteristics of surface potential to stress variation. The research results can provide an important experimental basis for squeezed branch piles for assessing concrete damage, identifying precursor characteristics of instability, and comprehensively grasping the damage evolution process and mechanical mechanism of concrete piles under load.

2. System, Sample, and Scheme for Squeezed Branch Piles Static Load Experiment

2.1. Test Measuring System

The experimental system for the surface potential of squeezed branch piles consists of a loading system and a potential data acquisition system (see Figure 1). The loading system is a self-made static load system of reaction beams. A static load is applied to the squeezed branch pile by the QJD2518005 vertical hydraulic jack so that squeezed branch piles can transmit and receive the load vertically.

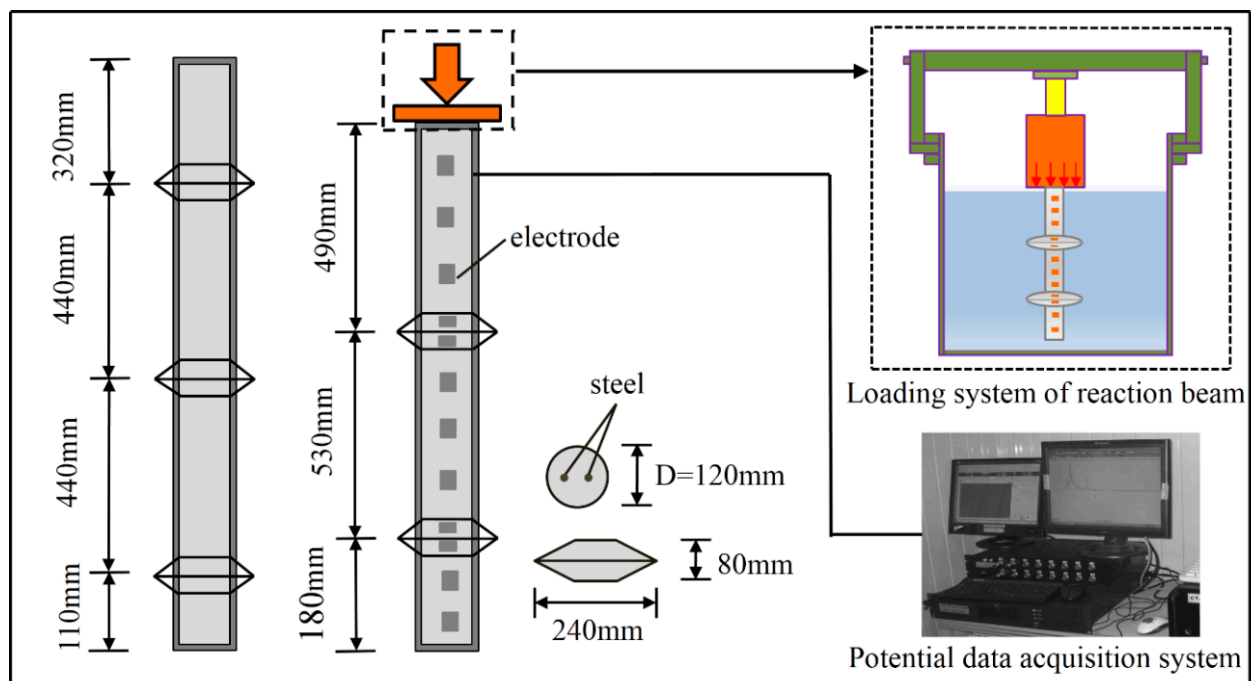


Figure 1. Schematic diagram of an experimental system for the surface potential of support piles.

The potential data acquisition system, which mainly consists of a data acquirer, a central control, and a front-end bridge amplifier, acquires potential-time data with the aid of the LB-IV data acquisition instrument. The data acquirer contains a main amplifier that allows the selection of 1, 2, 4, and 8 times magnification through programming.

- (1) The system has 16 signal channels with an analog-to-digital conversion resolution of 16 bits.
- (2) Signal sampling frequency can be selected between low-speed continuous sampling frequency (continuously adjustable in the range of 1–100 Hz) and high-speed continuous sampling frequency (adjustable in the range of 100–1000 Hz). The duration of the sampling frequency lies in the range of 1–200 s.
- (3) It has low system noise, which is not higher than 2/10,000 of the whole range under 40 dB conditions.
- (4) The amplification factor of a front-end bridge amplifier is 50 times. The generation of potential signals from the squeezed branch pile surface will change the balance of the bridge, and the system will sample the potential signals. In order to allow the bridge

to return to zero quickly after measuring a potential signal, a 5 M Ω discharge resistor is connected in parallel at the input end of the front-end amplifier. Besides the main amplifier can also allow the selection of 1, 2, 4, and 8 times magnification.

2.2. Composition of Experimental System

In order to obtain the bearing capacity of the branch pile under different numbers of branches, the squeezed branch pile model was poured into a pre-made mold and set up with two and three branches, respectively. The squeezed branch pile model concrete was arranged in the C40 grade with the diameter of aggregate controlled within 10 mm, and the mix ratio is cement:water:sand:stone = 1:0.47:1.59:3.39. Two steel bars with a diameter of 8 mm were placed in the pile body, while no steel bars were placed in the branches. The lengths of two-branch and three-branch piles were 1200 mm and 1350 mm, respectively; the diameters of pile and branch were 120 mm and 240 mm, respectively (see Figure 1).

Before the test, electrode sheets were attached to the corresponding positions of the squeezed branch pile models (see Figure 2). To minimize the interference of equipment with the surface potential of squeezed branch piles, insulating paper was padded on the contact surface between the squeezed branch piles and the jack. In this way, the influence of the loading system on the surface potential measurement results was reduced.

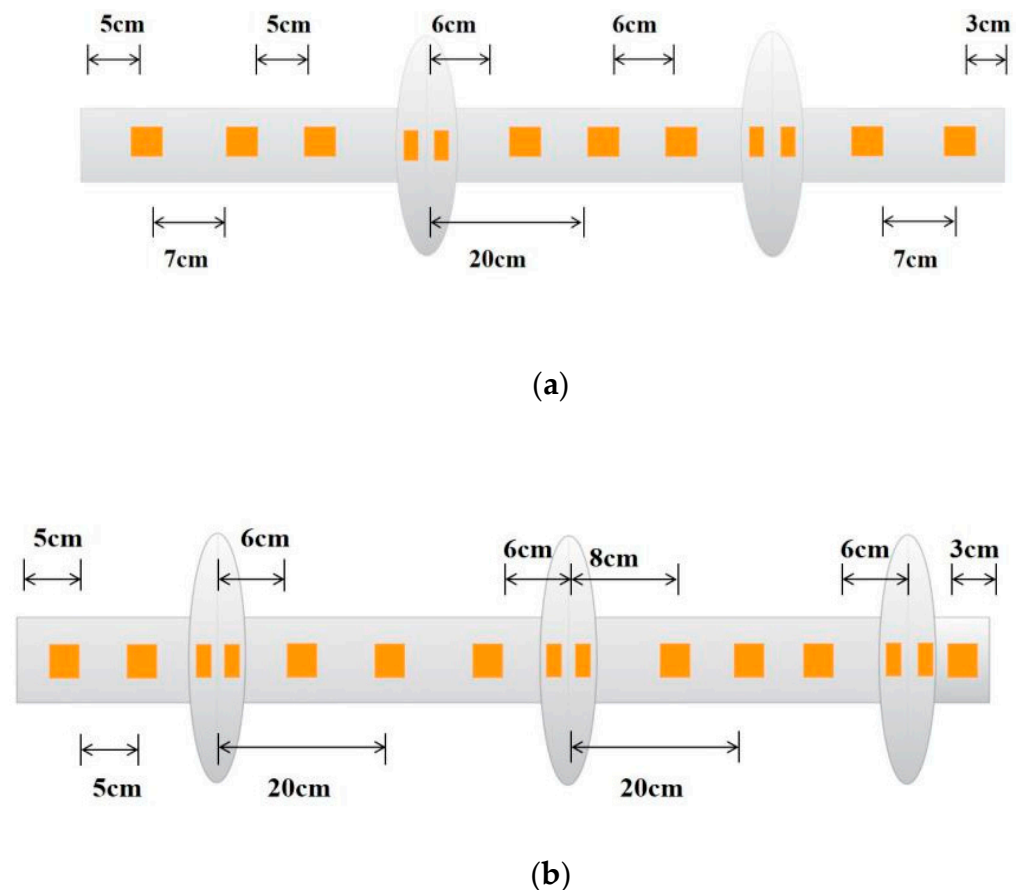


Figure 2. Potential sensor placement position of squeezed branch piles. (a) Potential sensor placement position of the two-branch pile; (b) Potential sensor placement position of the three-branch pile.

2.3. Static Load Test of the Squeezed Branch Pile Model

Under static load, the soil around the pile bears the axial load transmitted by the pile body in the form of friction and supporting force. As the upper load transfers from top to bottom, the soil around the pile shares part of the load in the form of side friction, whereas the load that is not completely offset by the side friction transfers to the bottom of the pile and applies to the soil layer at the pile bottom or branch. The static load test method

of reaction beam refers to the method that tests the bearing capacity of pile foundations by providing reaction force through platforms. In this experiment, graded loading was performed by using a jack as a force-exerting device. The loading was performed at 1 MPa per level, and each stress level was maintained for 60 s. The on-site test photos are shown in Figure 3.



Figure 3. Device for reaction beam loading.

2.4. Test Procedure

- (1) The tested squeezed branch pile was put between the self-made reaction beam and the jack, and insulation paper was placed on the pile top. Then, the experimental device was connected to the jack to start loading.
- (2) First, a certain initial force (1 MPa) was applied to the jack to help the jack, the reaction beam, and the squeezed branch pile enter a preliminary state of force stability.
- (3) The potential data acquisition system was turned on. The pre-acquisition of data began when the mean variance of the acquired data approached 0.
- (4) Next, graded loading was applied to the squeezed branch pile for 1 MPa and 60 s per level until the squeezed branch pile settled and failed completely.

3. Test Results

Eight representative potential channels were selected from the tested two-branch and three-branch piles, respectively, for analyzing the variation law of electrical signals, discussing the bearing characteristics of squeezed branch piles, and comparing the different fracture areas of the squeezed branch piles.

3.1. Characteristics of Surface Potential of a Two-Branch Pile under Load

The potential-time response characteristics of each part of a two-branch pile during the whole process of compression, cracking, and failure under axial load are displayed in Figure 4. It can be seen from Figure 4 that at the initial stage of loading (0–300 s), the side frictional resistance between the pile and the soil is small and the potential signal remains stable at a low value (80 mV). When the loading proceeds for about 290 s (axial stress: 5 MPa), the potential signals fluctuate violently for the first time. After that, in the second stage of loading, the amplitudes of potential channels 1 and 12 increase obviously with the continuous application of axial load. At this time, the jack that exerts axial compression destroys the pile top and thus damages the concrete structure, causing a pulse response of potential signals. When the loading progresses for 640 s (axial stress: 11 MPa), stable

low values of potential signals appear. At this time, the squeezed branch pile settles into a relatively stable position. When the loading proceeds for 670 s (axial stress: 12 MPa), high values of potential signals appear suddenly, and the breakage of the pile foundation makes a loud noise. Afterward, the squeezed branch pile enters the third stage of loading, where potential signals show stable low values due to the reduced settlement of the pile foundation that has become relatively stable in the soil. When the axial loading goes on for about 880 s (axial stress: about 15 MPa), stable low values of potential signals go upward. Finally, the phenomenon of high pulse response of potential signals is accompanied by the sound of concrete fracturing, which indicates breakage and instability of the pile body. As the last period prior to pile instability, the shortening of the stable low-value period of potential signals can be taken as a precursor feature of squeezed branch pile instability.

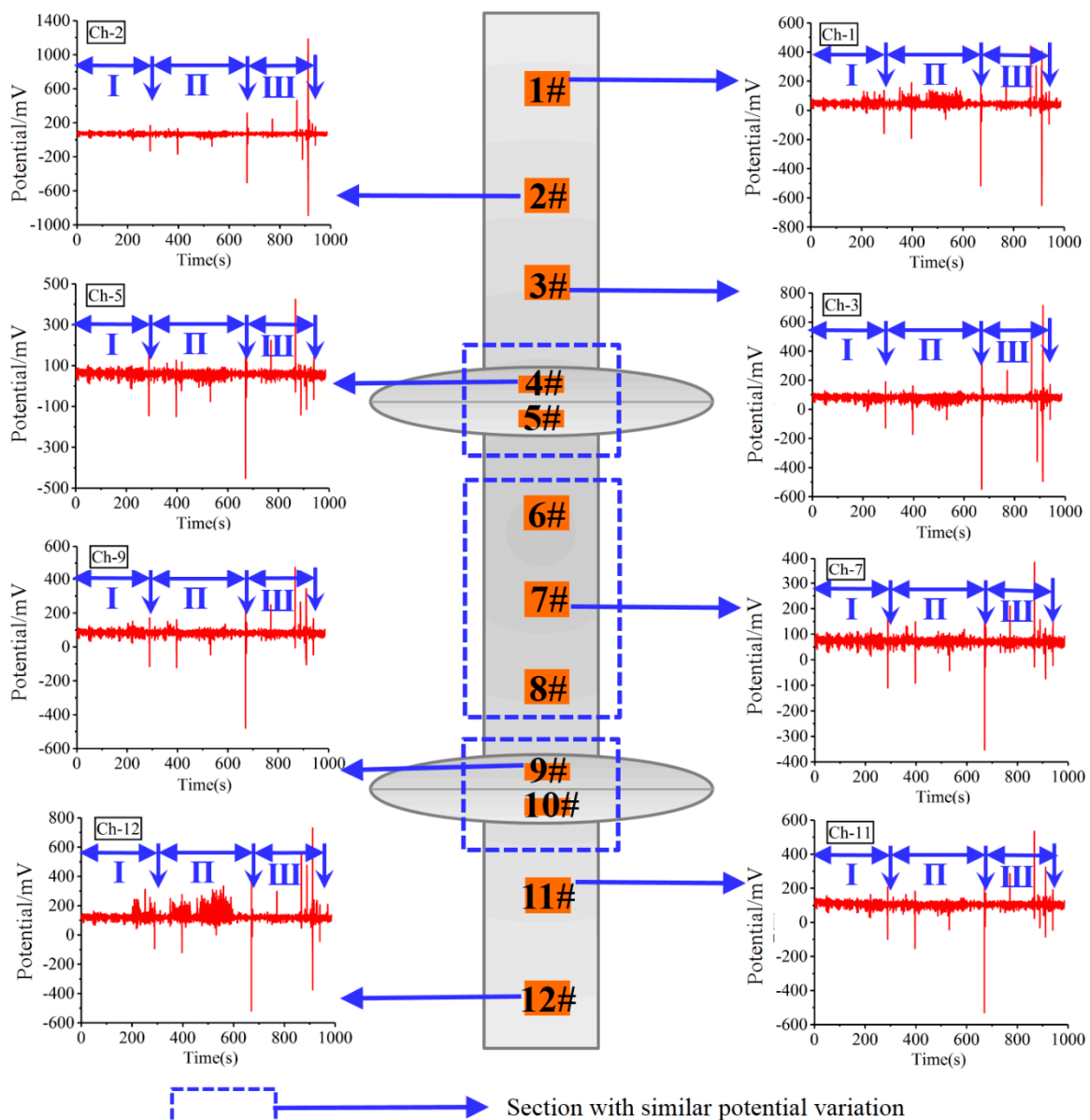


Figure 4. Experimental results of the surface potential of a two-branch pile (part of the channels).

3.2. Characteristics of Surface Potential of a Three-Branch Pile under Load

The potential-time response characteristics of a three-branch pile are exhibited in Figure 5. As can be observed from Figure 5, compared with the two-branch pile, it takes the three-branch pile a longer time to settle, deform, and lose stability. Besides the three-branch

pile has greater bearing capacity and “gentler” potential signals before instability. In the first stage of loading, the potential values acquired from potential monitoring channels all fluctuate within the range of 180–250 mV due to the settlement. When the loading proceeds for 320 s (axial stress: 6 MPa), the concrete structure of the pile body undergoes compressive deformation under axial load, and the potential signals surge for the first time. After that, the potential signals from the channels at the pile top and bottom fluctuate violently, while those from other channels restore the stable low value of the first stage. The overall increase in potential signal amplitude is not obvious. When the loading progresses for 970 s (axial stress: 17 MPa), the potential signals experience an obvious “gentle” period, which lasts for about 20 s before the signal rises again. At this time, the responses of all potential channels are consistent. Then, the high-value signal pulse appears along with the sound of concrete breaking. Compared with the two-branch pile, the third stage of the three-branch pile is relatively short, and its potential signals are “gentle” before instability. When the loading proceeds for 1000 s (the axial stress is 17 MPa), the “gentle” potential signals suddenly surge, accompanied by the sound of concrete pile breakage. Afterwards, the signals switch rapidly between the states of surging and stabilizing until they return to the stable low-value range, which indicates the complete instability of the pile foundation.

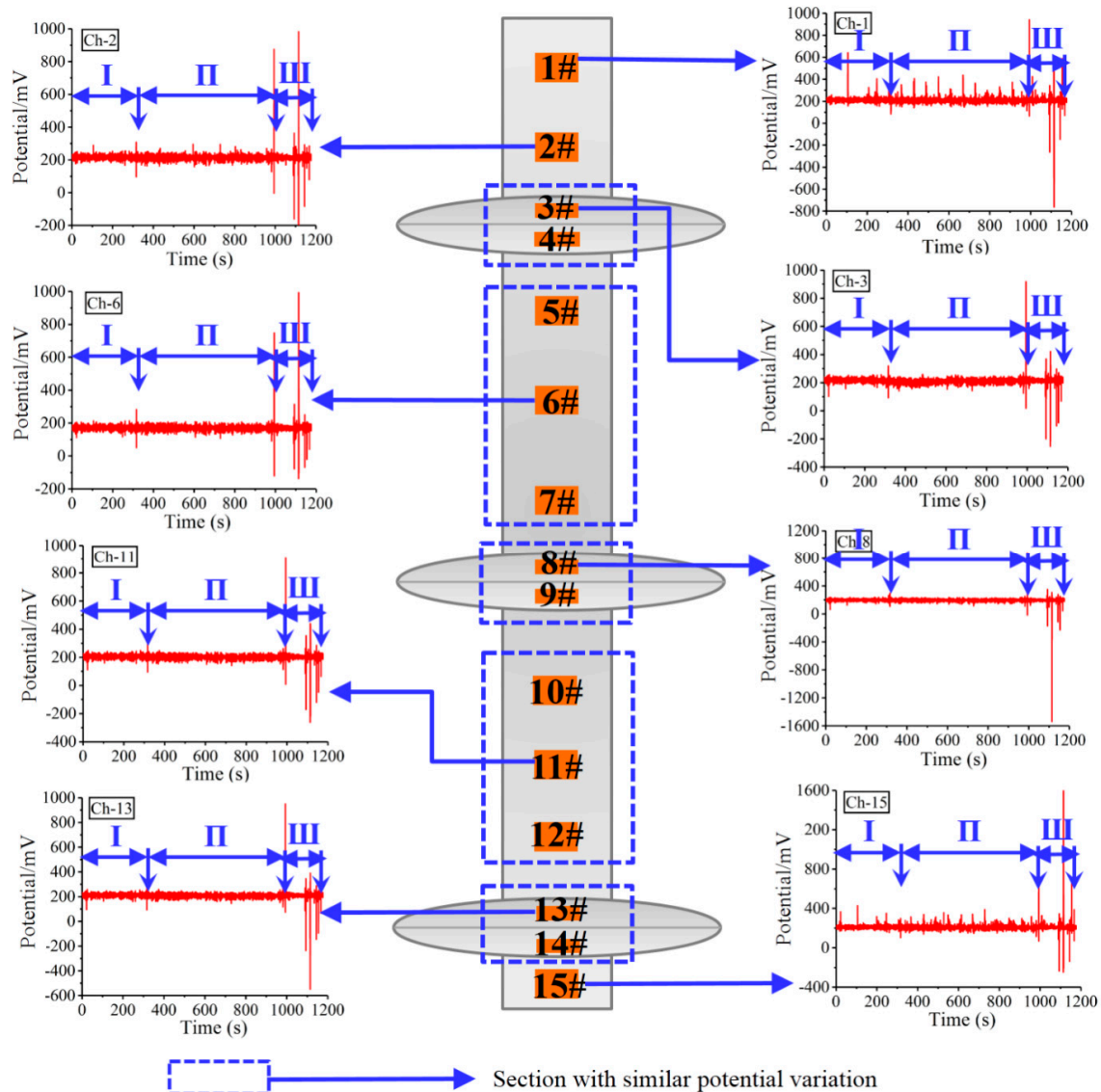


Figure 5. Experimental results of the surface potential of a three-branch pile (part of the channels).

3.3. Comparative Analysis of the Causes of Abnormal Surface Potential of Squeezed Branch Piles

The surface potential signal generated by the staged loading and compression failure of the squeezed branch piles is the result of the action of multiple potential signal sources. In terms of experimental phenomena, there is a certain difference between the surface potential of the squeezed branch piles and the surface potential of coal made by predecessors [27,28]. The concrete sample has a sudden increase in the amplitude of the surface potential before the peak of the principal stress and strain [27]; however, the surface potential of the coal sample basically increases with the increase of the load, and the potential signal has a good correlation with the stress and strain [28]. For the squeezed branch piles under staged loading, the process of settlement and failure is relatively complicated, so the mechanism of surface potential generation is relatively complicated. At different stages and in different areas, the dominant ways of generating free charge are different, so the dominant mechanism of abnormal surface potential signals is different. In order to better understand the cause of the abnormal surface potential signal of the squeezed branch piles, the different damage areas of the squeezed branch piles are selected for comparative analysis. (primary breaking region Ch-2, secondary breaking region Ch-5, and cracks at pile foundations Ch-12, Ch-15).

Comparing Figure 6a–c, it can be seen that the changing trend of the surface potential of the squeezed branch piles is closely related to the deformation and failure processes. The deformation and damage distribution of each squeezed branch pile is uneven, which leads to differences in the surface potential strength and change trend of different squeezed branch piles. The surface potential strength of different squeezed branch piles is different at the same time. The potential signal generated during the whole process of the three-branch pile due to the settlement effect is greater than that of the two-branch pile, and the potential signal difference in the cracks at the pile foundation is relatively small. During the entire rupture process, due to the greater bearing capacity of the three-branch pile, the two-branch pile requires 1000 s and the three-branch pile requires 1200 s, and the three-branch pile consumes a longer time in the second stage of the rupture. The fluctuation of the potential signal in the whole process of the primary breaking region is larger than that of the secondary breaking region and the cracks at the pile foundation. The overall potential signal fluctuation in the cracks at the pile foundation is relatively stable, and there is an obvious signal surge only before the instability of the squeezed branch pile is completely broken. It can be seen from (d) that the potential intensity of the cracks at the pile foundation is greater than the potential intensity of the primary breaking region and the secondary breaking region. At about 700 s, a high-value pulse signal appears in the cracks at the pile foundation, and at about 920 s, a high-value pulse signal appears in the primary breaking region. Around 900 s, a less obvious pulse signal appeared in the secondary breaking region. During the whole process, the secondary breaking region has no larger fluctuations than the other two regions.

A comprehensive analysis of the potential signal trends in different areas of the squeezed branch piles shows that the generation of potential signals has good regularity over time, and the potential signals at different positions are different, indicating that the potential has a good response to local rupture. The greater the number of branches, the better the bearing effect of the pile foundation and the smaller the settlement of the pile top.

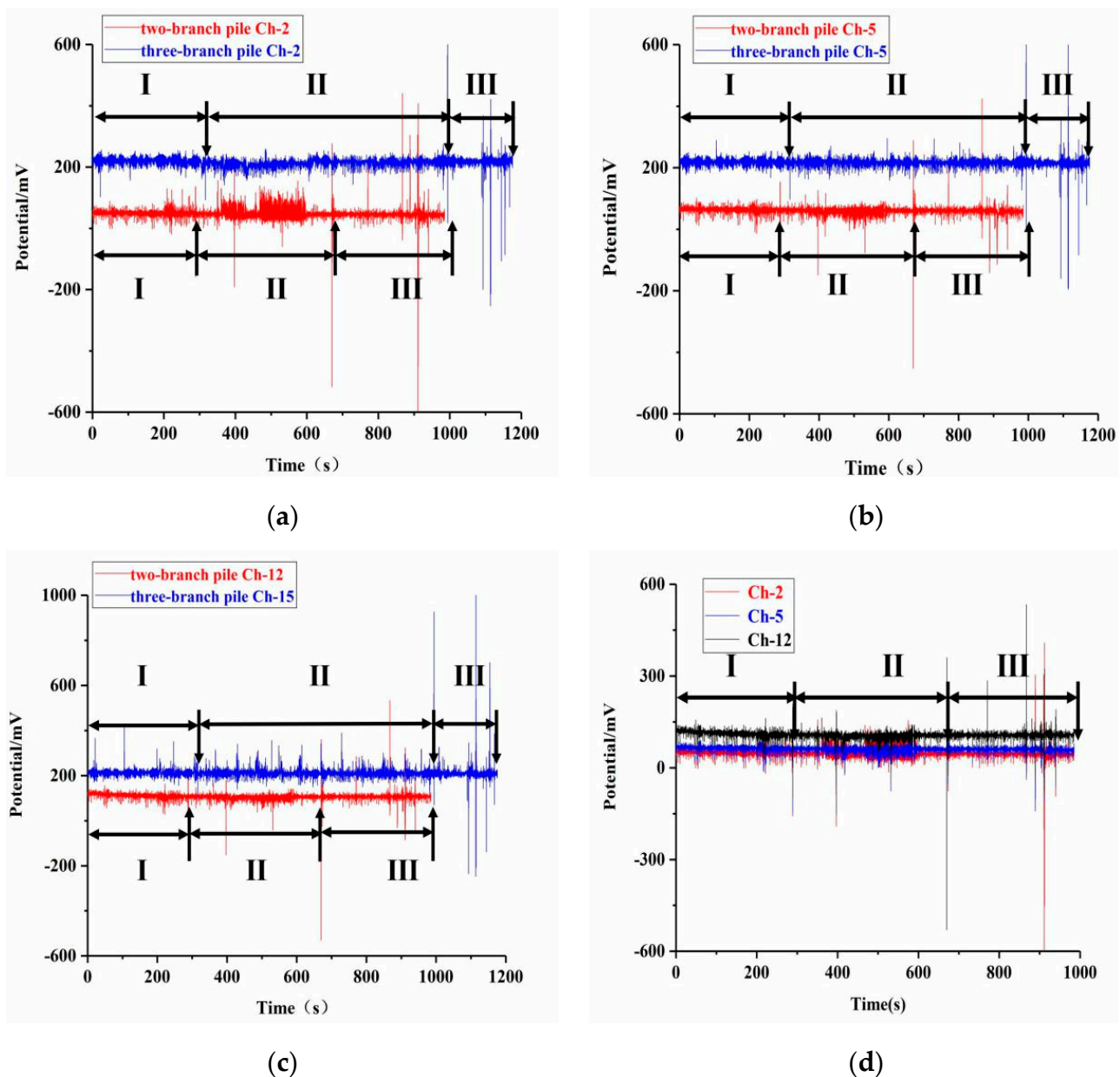


Figure 6. Comparative analysis of potentials in different damaged areas of squeezed branch piles. (a) Electrical signal of the primary breaking region; (b) Electrical signal of the secondary breaking region; (c) Electrical signal of cracks at the pile foundation; (d) Two-branch pile electric signal.

4. Discussion

4.1. Discharge Mechanism during Concrete Failure

In the process of concrete being loaded and deformed to failure, in the initial compression stage, a large number of holes and cracks in the concrete gradually compact and close as the load increases. In this process, the sliding friction between the hole and crack walls induces damage and failure of the internal structure of concrete, and the temperature of the friction surface increases. Accordingly, the electrical balance between concrete particles is broken, which causes free electromagnetic diffusion and leads to the generation of an electric charge. Meanwhile, the free charge generated by the compression of piezoelectric materials in concrete results in a change in surface potential [29,30] (The composition of concrete components is shown in Figure 7).

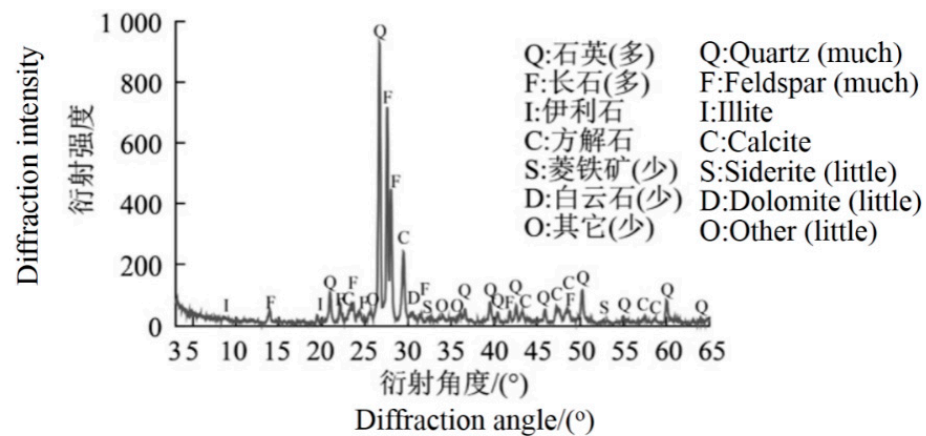


Figure 7. X-ray diffraction pattern of concrete [20].

As the loading progresses, the concrete enters the stage of elastic-plastic deformation. New cracks are generated when compression on the sample reaches the critical stress of crack propagation. Free electrons in the sample concentrate at crack tips [31,32]. On the one hand, positive and negative charges are generated at the crack tip to form an electric dipole; on the other hand, the new surface on both sides of the crack generates free charge. Due to the accumulation of electrons, the electron density and electric field strength at crack tips are the highest. The basic process of the discharge mechanism at crack tips in concrete is shown in Figure 8.

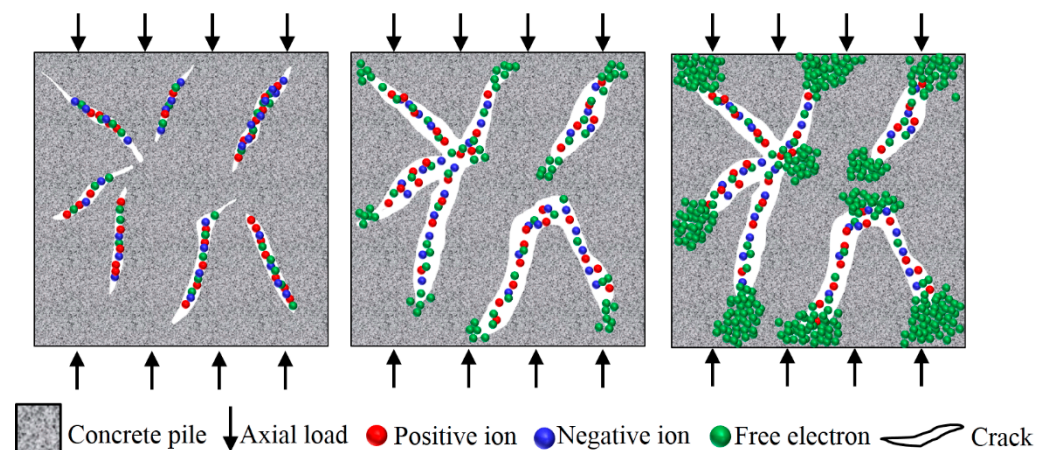


Figure 8. Discharge phenomenon at the crack tip of concrete.

Concrete is a kind of inhomogeneous material containing a large number of primary cracks and positive and negative charged ions. Under the action of axial load, micro-cracks in the sample expand and connect, and the free charges and newly generated charges accumulate at crack tips. The accumulation of numerous charges raises the density and number of charges. When the potential at crack tips reaches an electric field strength that is sufficient for discharge, many charges at crack tips are instantaneously released to the regions outside the tips, causing a local charging anomaly, which is manifested as a sudden increase in surface potential signals. While the electrons at the crack tips are released, the cracks expand to form new fracture surfaces, which also release new electrons. These electrons are emitted simultaneously with those enriched at crack tips, causing crack tips to exhibit a positive electrical characteristic of a potential signal in a short time. During charge enrichment at crack tips, conductive channels are formed as a result of charge movement. The surface potential signal shows pulse characteristics due to the flow of charges in the channels.

From the above analysis, it can be seen that concrete cracking is a process of micro-crack generation, expansion and connection, in which the movement and aggregation of

free electrons manifest as changes in surface potential signals. In contrast, large fracturing or even local instability of sample is the process in which a large number of free electrons accumulate and diffuse in a short time. This process leads to a local sudden change in electrical properties and macroscopically manifests as the pulse shape of potential signal. When the pile body remains in the state of continuous fracturing, the generation and expansion of cracks coexist, and the pulse shape of potential signal continues to appear.

4.2. Failure Mechanism of Squeezed Branch Piles and Response Characteristics of Potential Signals

The surface potential of squeezed branch piles is a macroscopic phenomenon of free charge movement during settlement, deformation, and failure of the pile body under axial load. The dominant mechanism of potential generation differs at different stages of pile foundation loading. In this section, the mechanism of surface potential generation is analyzed and discussed according to the above experiment.

In the initial stage of loading (the first stage), because the soil around the pile foundation is loose, the pile foundation mainly undergoes settlement under the action of axial load. The friction between the pile and the soil makes free charges on the surface of the pile foundation move directionally in a short time under the action of friction. As a result, a potential difference appears locally to generate the surface potential phenomenon. As the soil around the pile becomes dense and exerts greater resistance to the pile (the second stage), the weak structure of the pile body yields under the action of axial load and resistance, and the concrete fractures. At this time, free charges separated from the tips of newly generated cracks form an electric field under the action of tensile stress, resulting in the pulse signal of electric potential. The faster the new cracks generate in the pile, the more intensely the charges separate and concentrate, hence the stronger the electric field is and the higher the surface potential gets to some extent.

With the continuous increase in axial compression, when the pile foundation stays in a relatively stable position in the soil, the stress characteristics of squeezed branch piles under the test conditions can be roughly illustrated by Figure 9. The experimental device applies an axial load on the pile top through a reaction beam (an approximate simulation of axial force transmission in an actual pile). On the one hand, the compressed soil layer at the pile bottom produces normal force pointing to the pile bottom. On the other hand, it generates a tangential friction force on the contact surface with the pile bottom. The superposition of stresses between the branches is bound to affect the normal exertion of side friction force, whose value is bound to be smaller than that of a bored pile with the same diameter and length. Under the action of the load, the soil over the branch is in a void state, whereas the soil under the branch compacts and moves downward with the branch. Obviously, the friction resistance of the soil over the branch will decrease. Compared with common bored piles, the calculation of the bearing capacity of squeezed branch piles involves one more item, namely branch end resistance [32]. It consists of three items: pile side friction, pile end resistance, and branch resistance, i.e., According to the previous static load test [33], the load borne by the branch plate accounts for about 55% to 65% of the total load, while the pile side friction accounts for about 30% and the pile end resistance accounts for about 7%.

$$Q_k = \zeta Q_{sk} + Q_{pk} + \eta Q_{zk} = \zeta U \sum_{q_{ski}} L_i + q_{pk} A_p + \eta \sum_{q_{ski}} A_{zi} \quad (1)$$

where Q_k is the standard value of the vertical ultimate bearing capacity of a single pile; Q_{sk} is the total side frictional resistance (kN); Q_{zk} is the total branch end resistance (kN); Q_{pk} is the pile end resistance (kN); U is the circumference of pile (m); L_i is the average effective thickness of the i th layer on the pile side; A_p is the pile end area (m²); ζ the frictional resistance coefficient that is smaller than 1 (related to the construction process, the nature of the soil layer on the side of the pile and the spacing between the branches and plates); η is the correction coefficient of branch end resistance (related to the compaction effect of the squeezing equipment on each layer of soil, the size effect of the bearing plate and the net spacing of the branch plates); q_{skj} is the standard value of ultimate friction resistance of the j th pile (kPa); q_{zki} the standard value of ultimate end resistance of the soil at the i th

branch (kPa); q_{pk} is the standard value of ultimate bearing capacity of the pile end (kPa); and A_{zi} is the projected area of branch on the horizontal plane. Therefore, a correction factor greater than one should be multiplied in the calculation of branch end resistance. As for the selection of ζ and η values, the spacing between branches and the properties of soil should be taken into account, and the functional relationship between them and these factors should be established based on a large number of measured data points.

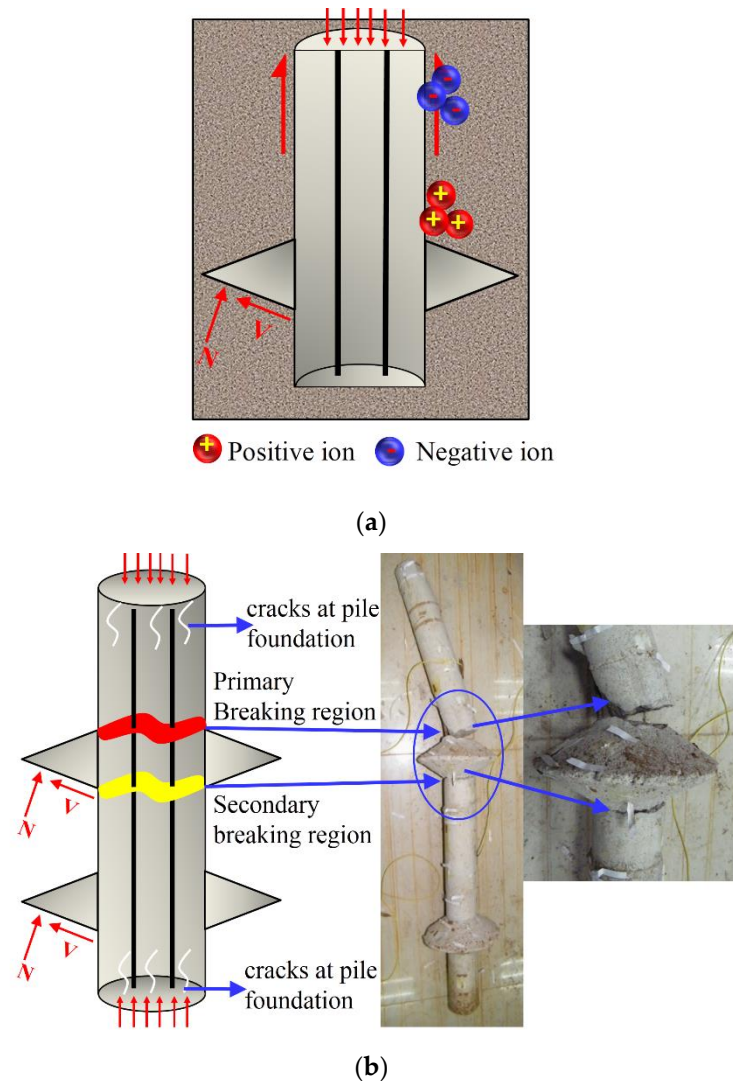


Figure 9. Mechanism of the potential generation of branch piles. (a) Mechanism of potential generation by friction; (b) Mechanism of potential generation by cracking.

In the loading process, the branch forms an uneven axisymmetric three-dimensional stress field near the straight pile connected to its upper and lower sides under the action of external force. With the progress of graded loading, stress on the upper part of the pile increases continuously. At this time, newly generated cracks in the pile are partially penetrated and connected under the continuous action of stress, leading to the formation of a pressing area within a certain range. The failure of branch piles occurs when the area reaches the damage limit of the pile. According to the observation of the damaged pile body, the pile generates a large tensile stress along the circumferential direction of the lower surface under the axial load and forms a certain angle with the axial stress. Consequently, the pile body at the connection point between the branch and the vertical pile is subjected to the action of axial stress and shear force. When its tensile stress reaches the ultimate tensile strength of concrete or when the elongation deformation reaches the ultimate tensile

strain of concrete, the pile cracks first in this region, and the crack rapidly expands as the load increases. As presented in Figure 9b, the upper branch at the joint of stress exertion and settlement resistance in the experiment was found that the upper and lower parts of upper branch are the main position of pile deformation and fracturing. When the loading reaches the ultimate load (peak load), the potential signals fluctuate significantly, and the peak pulse phenomenon appears in the potential signal. The experimental phenomenon at this time is the sound of branch piles fracturing. The continuously increasing axial load eventually leads to complete damage to the pile body, and the fractured site of the pile foundation exhibits obvious crushing characteristics.

5. Conclusions

In this study, the method of model test and conclusion analysis is used to study the surface potential characteristics of squeezed branch pile stress models through test and analysis. The variation characteristics of the surface potential of the two-branch pile and the three-branch pile under load are analyzed, and the different damage areas of the branch piles are compared and analyzed. The failure mechanism and concrete discharge mechanism of squeezed branch piles under load are discussed. According to the observation and discussion, the following conclusions are drawn:

- (1) Surface potential signals are generated during the deformation of squeezed branch piles under load, and the deformation state of the pile body is the dominant factor affecting the surface potential signals. In the initial stage of loading, the squeezed branch piles get compressed and settle under the action of axial load, and potential signals fluctuate in a small range with the increase in of load. With the increase in load on the pile top, the weak structure of the test pile yields, and the peak pulse phenomenon appears in the potential signal. With the further increase in load, the upper branch of squeezed branch piles broke due to the interaction between the pile and the soil. At this time, the peak pulse frequency of potential signals increases, and the potential signal responds with large values.
- (2) During the whole static load simulation test on the squeezed branch piles, the changes in surface potential signals are well correlated with the load on the pile top, the deformation of pile body and the setting of branches. Therefore, the changes in surface potential signals can be used to predict the deformation and failure state of squeezed branch piles and to further evaluate the stress state and stability of squeezed branch piles. This finding provides a new method and means for quality detection and damage assessment of branch piles.
- (3) The change in surface potential signal is the macroscopic manifestation of pile settlement, deformation, and free charge movement. The failure of concrete under load causes a change in the surface potential signal caused by free electrons generated by friction electrification, piezoelectric effect, crack propagation, and charge separation under non-equilibrium stress.

Author Contributions: Conceptualization, S.Z.; Methodology, S.Z.; Validation, X.L.; Investigation, Y.N.; Resources, H.Z.; Data curation, H.Z.; Writing—original draft, S.Z. and X.L.; Writing—review & editing, X.L. and C.P.; Supervision, H.Z., C.P. and Y.N. All authors have read and agreed to the published version of the manuscript.

Funding: This research was supported by the National Natural Science Foundation of China, grant number (52174218, 51774280), and the Science and Technology Planning Project of Guizhou Province, China (No. [2022] General 078).

Data Availability Statement: The data presented in this study are available on request from the corresponding author. The data are not publicly available due to the article data involves privacy and is currently inconvenient to disclose.

Acknowledgments: The authors are grateful to all the people who help us in this paper.

Conflicts of Interest: The authors declare no conflict of interest.

References

1. Jiang, Q.Q.; Meng, Q.L.; Hu, Y.F.; Lai, W. Engineering application of settlement-controlled composite pile foundations. *Chin. J. Rock Mech. Eng.* **2008**, *27*, 3153–3158.
2. Yang, J.P.; Piao, C.D. Distributed detection and bearing mechanism of squeezed branch piles. *Chin. J. Geotech. Eng.* **2013**, *35*, 1232–1235.
3. Pradhan, M.K.; Kumar, P.; Phanikanth, V.S.; Choudhury, D.; Srinivas, K. A review on design aspects and behavioral studies of pile foundations in liquefiable soil. *Geomech. Geoengin.* **2023**, *18*, 347–379. [[CrossRef](#)]
4. Liu, X.D.; Li, H.C.; Zhao, J.L. Code for design of highway bridge and culvert foundation and foundation (JTG3363-2019) Introduction to the revision. *Highway* **2021**, *66*, 162–164.
5. Wang, Y.M.; Zhang, K.B.; Qiu, S.; Chen, Y.K.; Xu, D.J.; Yang, J.P. Comparative study on the design parameters and compressive bearing capacity of squeezed branch piles based on current specifications. *Build. Struct.* **2023**, *53*, 2648–2653.
6. Lueprasert, P.; Jongpradist, P.; Jongpradist, P.; Suwansawat, S. Numerical investigation of tunnel deformation due to adjacent loaded pile and pile-soil-tunnel interaction. *Tunn. Undergr. Space Technol.* **2017**, *70*, 166–181. [[CrossRef](#)]
7. Su, Q.Q.; Xia, H.B.; Wu, K.M.; Yang, F.L.; Pascoletti, G. The Effects of Branch Spacing and Number on the Uplift Bearing Capacity of a New Squeezed Multiple-Branch Pile: A Numerical Simulation Analysis. *Model. Simul. Eng.* **2023**, *2023*, e3758253. [[CrossRef](#)]
8. Zhang, M.X.; Xu, P.; Cui, W.J.; Gao, Y.B. Bearing behavior and failure mechanism of squeezed branch piles. *J. Rock Mech. Geotech. Eng.* **2018**, *10*, 935–946. [[CrossRef](#)]
9. Chen, F.; Wu, K.X.; He, S. Field tests on load transfer performances of squeezed branch piles. *Chin. J. Geotech. Eng.* **2013**, *35*, 990–993.
10. Wang, Y.; Xu, L.; Li, B.; Xu, C. Finite element numerical study on the axial bearing behaviors and factors of squeezed branch pile. *China Civ. Eng. J.* **2015**, *48*, 158–162.
11. Wang, E.Y.; Liu, X.F.; He, X.Q.; Li, Z.H. Acoustic emission and rock dynamic and electromagnetic radiation synchronized monitoring technology and early-warning application for coal and rock disaster. *J. China Univ. Min. Technol.* **2018**, *47*, 942–948.
12. Liu, X.F.; Zhang, S.Q.; Wang, E.Y.; Zhang, Z.; Wang, Y.; Yang, S. Multi-Index Geophysical Monitoring and Early Warning for Rockburst in Coalmine: A Case Study. *Int. J. Environ. Res. Public Health* **2023**, *20*, 392. [[CrossRef](#)] [[PubMed](#)]
13. Liu, X.; Zhang, H.; Wang, X.; Zhang, C.; Xie, H.; Yang, S.; Lu, W. Acoustic Emission Characteristics of Graded Loading Intact and Holey Rock Samples during the Damage and Failure Process. *Appl. Sci.* **2019**, *9*, 1595. [[CrossRef](#)]
14. Behnia, A.; Chai, H.K.; Shiotani, T. Advanced structural health monitoring of concrete structures with the aid of acoustic emission. *Constr. Build. Mater.* **2014**, *65*, 282–302. [[CrossRef](#)]
15. Zhang, Z.; Wang, E.; Zhang, H.; Bai, Z.; Zhang, Y.; Chen, X. Research on nonlinear variation of elastic wave velocity dispersion characteristic in limestone dynamic fracture process. *Fractals* **2023**, *31*, 2350008. [[CrossRef](#)]
16. Zhang, Z.B.; Wang, E.Y.; Li, N.; Zhang, H.; Bai, Z.; Zhang, Y. Research on macroscopic mechanical properties and microscopic evolution characteristic of sandstone in thermal environment. *Constr. Build. Mater.* **2023**, *366*, 13015. [[CrossRef](#)]
17. Li, Z.H.; Cheng, F.Q.; Wei, Y.; Cao, K.; Zhang, X.; Zhang, Y.; Tian, H.; Wang, X. Study on coal damage evolution and surface stress field based on infrared radiation temperature. *J. Geophys. Eng.* **2018**, *15*, 1889–1899. [[CrossRef](#)]
18. Hiasa, S.; Birgul, R.; Catbas, F.N. A data processing methodology for infrared thermography images of concrete bridges. *Comput. Struct.* **2017**, *190*, 205–218. [[CrossRef](#)]
19. Watanabe, A.; Tokuda, S.; Mizuta, Y.; Miyamoto, S.; Nakanishi, T.; Furukawa, H.; Minagawa, H. Toward automated non-destructive diagnosis of chloride attack on concrete structures by near infrared spectroscopy. *Constr. Build. Mater.* **2021**, *305*, 124796. [[CrossRef](#)]
20. Liu, Z.T.; Li, X.L.; Li, Z.H.; Liu, Y.J.; Yang, L.Y.; Feng, J.J. Electric potential of the hole wall of concrete under uniaxial compression. *Meitan Xuebao/J. China Coal Soc.* **2014**, *39*, 372–377.
21. Wang, E.Y.; Li, Z.H.; Liu, Z.T.; Li, Y.N.; Song, X.Y. Experimental study on surface potential effect of coal under load. *Chin. J. Geophys.* **2009**, *52*, 1318–1325. (In Chinese) [[CrossRef](#)]
22. Niu, Y.; Li, Z.H.; Kong, B.; Wang, E.; Lou, Q.; Qiu, L.; Kong, X.; Wang, J.; Dong, M.; Li, B. Similar simulation study on characteristics of electric potential response to coal mining. *J. Geophys. Eng.* **2017**, *15*, 42–50. [[CrossRef](#)]
23. Li, Z.H.; Wang, E.Y.; Liu, Z.T.; Song, X.Y.; Li, Y.N. Study on characteristics and rules of surface potential during coal fracture. *J. China Univ. Min. Technol.* **2009**, *38*, 187–192.
24. Li, Z.; Niu, Y.; Wang, E.; Liu, L.; Wang, H.; Wang, M.; Ali, M. Experimental Study on Electric Potential Response Characteristics of Gas-Bearing Coal During Deformation and Fracturing Process. *Processes* **2019**, *7*, 72. [[CrossRef](#)]
25. Pan, Y.S.; Tang, Z.; Li, Z.H.; Zhu, L.-Y.; Li, G.-Z. Research on the chargeinducing regularity of coal rock at different loading rate in uniaxial compression tests. *Chin. J. Geophys.* **2013**, *56*, 1043–1048.
26. Xiao, Q.; Wang, D.H.; Xu, J. Experimental study on mechanical characteristics of squeezed branch pile of transmission line. *J. Exp. Mech.* **2015**, *30*, 124–130.
27. Li, Z.; Niu, Y.; Wang, E.; He, M. Study on electrical potential inversion imaging of abnormal stress in mining coal seam. *Environ. Earth Sci.* **2019**, *78*, 255. [[CrossRef](#)]
28. Yin, S.; Li, Z.H.; Niu, Y.; Qiu, L.M.; Sun, Y.H.; Chen, F.Q.; Wei, Y. Experimental study on the characteristics of potential for coal rock evolution under loading. *J. China Coal Soc.* **2017**, *42*, 9–103.

29. Ren, X.K.; Wang, E.Y.; Li, Z.H. Experimental study of characteristics of surface potential and electromagnetic radiation of pre-cracked rock plate during fracture. *J. China Univ. Min. Technol.* **2016**, *45*, 440–446.
30. Hao, J.Q.; Liu, L.Q.; Long, H.L.; Ma, S.L.; Guo, Z.Q.; Qian, S.Q.; Zhou, J.G. New result of the experiment on self-potential change of rocks under biaxial compression. *Chin. J. Geophys.* **2004**, *47*, 475–482. (In Chinese) [[CrossRef](#)]
31. Liu, J.; Liu, S.D.; Cao, Y. Self-potential characteristics in deep rock mass damage based on point discharge mechanism. *Chin. J. Geophys.* **2018**, *61*, 323–330.
32. Ju, Y.W.; Liang, R.W.; Bai, X.H.; Zhang, S.Y. Experimental study on the failure pattern of expanded plates of the squeezed branch pile. *Eng. Mech.* **2013**, *30*, 188–194.
33. Qian, D.L. Study on bearing behavior of squeezed branch pile. *Chin. J. Rock Mech. Eng.* **2003**, *22*, 494–499.

Disclaimer/Publisher’s Note: The statements, opinions and data contained in all publications are solely those of the individual author(s) and contributor(s) and not of MDPI and/or the editor(s). MDPI and/or the editor(s) disclaim responsibility for any injury to people or property resulting from any ideas, methods, instructions or products referred to in the content.